HIGH-EFFICIENCY AMORPHOUS SILICON ALLOY BASED SOLAR CELLS AND MODULES

Quarterly Technical Progress Report
June 1, 2003 through August 31, 2003

S. Guha and J. Yang
United Solar Ovonic Corp.
Troy, Michigan

NREL Technical Monitor: Bolko von Roedern

Prepared under Subcontract No. ZDJ-2-30630-19

1. Overview

In Phase I, we have carried out studies of hydrogenated microcrystalline silicon (μc-Si:H) solar cell as a substitute for hydrogenated amorphous silicon germanium alloy (a-SiGe:H) bottom cell in amorphous silicon (a-Si:H) based multi-junction structures and achieved an initial active-area efficiency of 13.0% using an a-Si:H/μc-Si:H double-junction structure and 12.2% using an a-Si:H/a-SiGe:H/μc-Si:H triple-junction structure. Compared to the best multi-junction cells using μc-Si:H as bottom cell made by Kaneka [1] and Canon [2], our main shortcoming is low short-circuit current density (J_{sc}). Normally, we obtain total current density of 24-25 mA/cm^2 for a multi-junction cell from quantum efficiency measurements, which is remarkably lower than the values ~30 mA/cm^2 reported by Kaneka [1] and Canon [2]. Many factors can contribute to the lower J_{sc}. We identified two predominant issues that affect the J_{sc}. One is that the intrinsic μc-Si:H layer is too thin to generate high current density. The second is that the Ag/ZnO back reflector (BR) is not optimized for best light-trapping effect and, further, it causes a problem called microcrystallite collision. As previously reported, we could not obtain high J_{sc} by increasing cell thickness for single-junction μc-Si:H solar cells. That was attributed to the occurrence of microcrystallite collision for thick films on BR's with high texture and/or to the increase of microcrystalline volume fraction with film thickness. A high microcrystalline volume fraction is normally associated with high microvoid or microcrack density, a factor that causes impurity diffusion and ambient degradation. In order to have a better understanding for the low J_{sc}, we have carried out systematic studies of thickness dependence of μc-Si:H cell performance and hydrogen dilution profiles.

We continued on the optimization of high rate deposition of μc-Si:H solar cells using MVHF and achieved a μc-Si:H single-junction cell with an initial active-area efficiency of 7.7% and an a-Si:H/μc-Si:H double-junction cell with an initial active-area efficiency of 11.9%, where the bottom cell μc-Si:H intrinsic layer was deposited in 40 minutes. In addition, we started high rate μc-Si:H deposition using RF glow discharge under high pressure and high power condition and achieved an initial active-area efficiency of 12.3% using a-Si:H/μc-Si:H double-junction structure.

For large-area deposition, we improved thickness uniformity by using a new cathode design during Phase I. In this quarter, we optimized the deposition conditions under the constraints of the production machine and achieved an initial active-area efficiency of 11.4% using SiH_4 and GeH_4 mixture instead of Si_2H_6 and GeH_4 mixture.

2. Thickness dependence of μc-Si:H single-junction cell

For μc-Si:H solar cells, due to the indirect optical transition in microcrystallites, the absorption coefficients are not high enough to generate high current density with a thickness less than 1 μm. Therefore, an optimized back reflector with a textured surface is very important for increasing cell efficiency by light trapping effects. However, microcrystallites are normally formed with columnar structure perpendicular to the substrate surface. On a textured surface, microcrystallite collision occurs when the film thickness is greater than a certain value, which leads to increased microvoid density and

defect density at the grain boundaries, and, thereby, deteriorates the performance of μc-Si:H solar cells. On the other hand, μc-Si:H deposition is an inhomogeneous growth process. The microstructure evolves with increasing thickness when the same growth conditions are used during deposition. It has been shown that μc-Si:H material and solar cell performance critically depend on the structure of microcrystallites. Dense and compact materials are normally deposited under the condition just over the microcrystalline/amorphous transition. Materials with high microcrystalline volume fraction and large grains normally have high microvoid and microcrack density, which allow impurities to diffuse into the material and cause poor solar cell performance. In order to identify the main problem for low J_{sc}, we carried out a systematic study of thickness dependence of solar cell performance.

Two sets of μc-Si:H single-junction solar cells were made using MVHF glow discharge with different intrinsic layer thicknesses. One set was made on textured Ag/ZnO coated stainless steel (BR), and another on specular stainless steel (SS). The same growth recipe was used for both sets of solar cells on the different substrates. The thickness of the samples was obtained using optical method. The thickness showed a linear dependence on deposition time and confirmed a constant deposition rate. We found that the deposition rates are the same on SS and BR. If microcrystallite collision is the main cause for low J_{sc}, the cell performance on a flat substrate (SS) would exhibit less deterioration of cell performance with increase in thickness since microcrystallite collision is characteristic of textured surface. However, if the results are otherwise, the increase of microcrystalline volume fraction with thickness would be the main problem.

Table I lists the J-V characteristics of μc-Si:H solar cells deposited on BR substrate with different intrinsic layer thickness. One can see that the J_{sc}, calibrated by quantum efficiency measurement, increases with increasing thickness up to ~1.0 μm, and then saturates. For the cell with thickness ~2 μm, the J_{sc} is lower than that for the cell with thickness ~1 μm. Both V_{oc} and FF decrease monotonically with increasing thickness. The overall cell efficiency reaches a maximum for the thickness ~1 μm. Figure 1 (a) plots the quantum efficiency (Q) of the six cells. One can see that for cells with thin μc-Si:H intrinsic layer, the long wave length response increases with cell thickness; but for the cell with ~2 μm thick intrinsic layer, the response at the middle and long wavelength region is lower than that for the 1 μm thick cell. The significant

Table I. J-V characteristics of μc-Si:H cells deposited using MVHF on BR with different thicknesses, where FF_b and FF_r represent the fill factor under blue and red light.

Run No.	Thickness (nm)	J_{sc} (mA/cm^2)	V_{oc} (V)	FF	P_{max} (mW/cm^2)	FF_b	FF_r
12116	290	16.41	0.503	0.638	5.27	0.620	0.610
12120	493	19.77	0.476	0.633	5.96	0.626	0.636
12121	940	23.25	0.443	0.585	6.03	0.617	0.620
12119	990	22.47	0.436	0.612	6.00	0.628	0.619
12122	1340	23.23	0.424	0.533	5.25	0.568	0.597
12124	1930	21.80	0.392	0.491	4.20	0.521	0.569

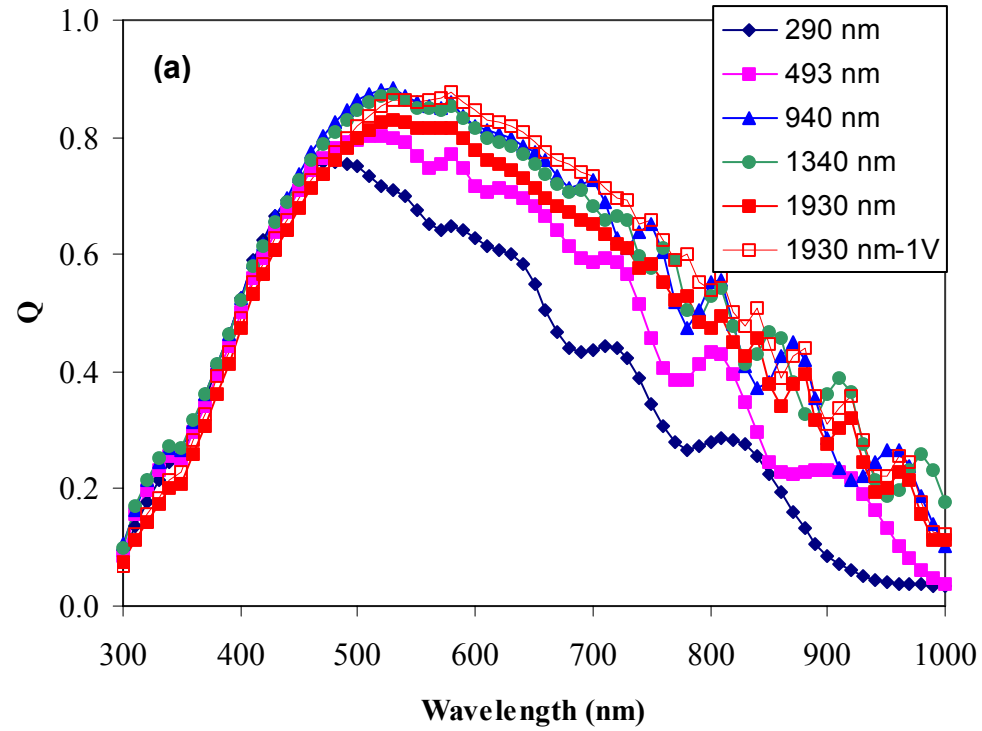

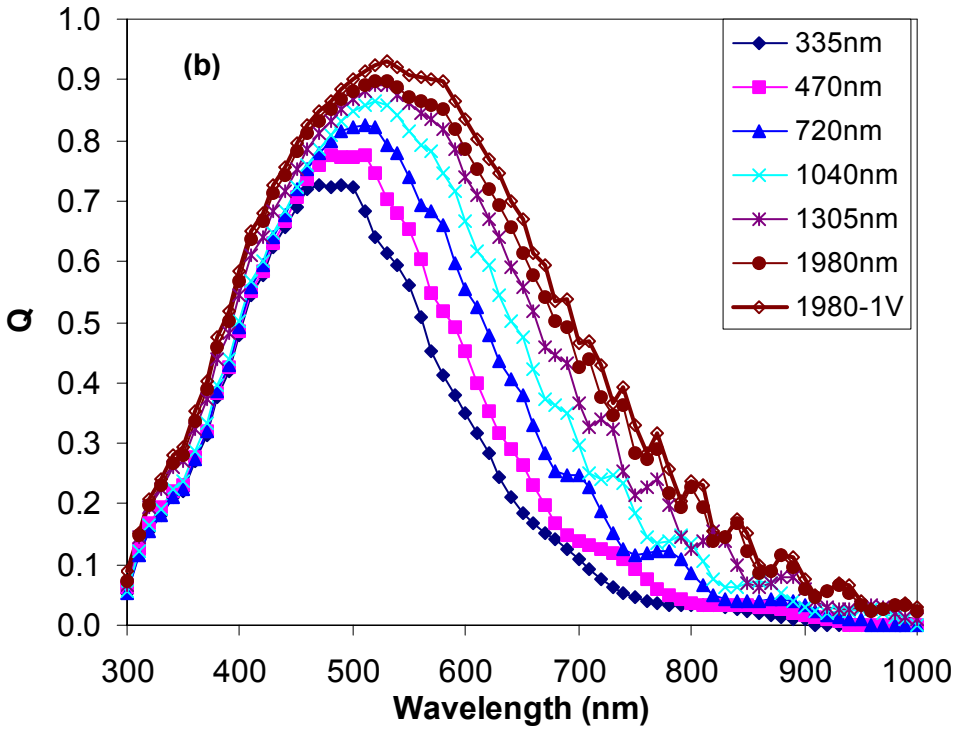

Figure 1. Quantum efficiency of μc-Si:H cells deposited using MVHF on (a) BR and on (b) SS with different thicknesses.

increase of quantum efficiency under reverse bias indicates an insufficient collection, which could be related to high recombination due to defects in the intrinsic layer.

Table II lists the J-V characteristics of the μc-Si:H solar cells on SS made with the same recipe as corresponding cells deposited on BR as listed in Table I. One can see that the behavior of the V_{oc} and FF versus thickness is similar to that on BR. However, J_{sc} keeps increasing up to a thickness of ~2 μm. Compared to cells with the same thickness on BR, cells on SS have lower J_{sc} and V_{oc}, but better FF. From Fig. 1 (b), one can observe the continuous increase of the long wavelength response with thickness of cells on SS. The difference between the reverse biased quantum efficiency and the quantum efficiency under short-circuit condition is much smaller for the 2 μm cell on SS than on BR, which implies that the cell on SS has less problem of carrier collection than the one on BR.

Due to the smooth substrate, light absorption in the cells on SS is much less than those on BR for the same thickness. This leads to a lower J_{sc}. In addition, the low light absorption causes only a narrow splitting of the Fermi levels, which gives rise to low V_{oc}. Further, the narrow Fermi level splitting reduces the recombination of the excited carriers, which results in a high FF for cells on SS, and hence less difference between the zero and negative biased quantum efficiency. A fair comparison about V_{oc} and FF for cells on different substrates should be under similar J_{sc}, instead of same light intensity. In this case, we expect a similar splitting of Fermi levels. For this purpose the solar cells on BR was measured with reduced light intensities to generate similar current densities to the solar cells on SS by using neutral filters. Table III lists J-V characteristics of four pairs of solar cells with different thicknesses. The two cells in each pair have a similar thickness, but one on BR and the other on SS. One can see that when the solar cells on BR were adjusted to have a current density similar to those on SS, the V_{oc} and FF also become very similar. This indicates that the BR substrate used at out lab does not have a pronounced effect on the carrier transport in μc-Si:H solar cell. In conclusion, we found that the microcrystallite collision for cells on BR could be a partial reason for low J_{sc}, but it is not the main factor. Therefore, the other mechanism of increase of microcrystalline volume fraction with increasing thickness could be responsible for the low J_{sc}.

The transition from amorphous to microcrystalline regime is accompanied by a change of surface morphology, especially roughness. Within the microcrystalline regime, the surface morphology also changes with the growth of grains. In order to

Table II. J-V characteristics of μc-Si:H solar cells deposited using MVHF on SS with different thicknesses, where FF_b and FF_r represent the fill factor under blue and red light.

Run No.	Thickness (nm)	Q (mA/cm^2)	V_{oc} (V)	FF	P_{max} (mW/cm^2)	FF_b	FF_r
12129	335	9.45	0.47	0.651	2.89	0.650	0.668
12125	470	10.98	0.466	0.672	3.44	0.664	0.670
12127	720	12.99	0.439	0.640	3.65	0.608	0.627
12123	1040	14.80	0.434	0.621	3.99	0.649	0.655
12128	1305	16.51	0.414	0.578	3.95	0.615	0.632
12126	1980	17.87	0.393	0.510	3.58	0.584	0.612

Table III. Comparison of the solar cell performance on different substrates. For the measurements of cells on BR, the light intensity was adjusted, using neutral density filters, to yield a J_{sc} similar to that of cells on SS.

Thickness (nm)	Substrate	J_{sc} (mA/cm^2)	V_{oc} (V)	FF	P_{max} (mW/cm^2)
470	BR	11.7	0.451	0.646	3.42
	SS	11.8	0.467	0.669	3.69
1040	BR	15.4	0.421	0.636	4.12
	SS	15.6	0.435	0.623	4.22
1305	BR	17.0	0.413	0.551	3.88
	SS	17.5	0.416	0.579	4.22
1980	BR	18.7	0.385	0.501	3.61
	SS	18.8	0.395	0.508	3.76

observe such changes on the top surface of solar cells with different thicknesses, twelve μc-Si:H solar cells with different thicknesses were sent to NREL for Atomic Force Microscope (AFM) measurements. Figure 2 shows three AFM images of (upper) a SS substrate, (middle) a 0.3 μm thick μc-Si:H solar cell on SS, and (bottom) a 2 μm thick μc-Si:H cell on SS. It appears that the size of the hill-like features on the top surface of the μc-Si:H cell increases with cell thickness. Also, the hill-like features have more structure. We believe that these hill-like features are clusters of microcrystalline grains. The AFM images of the μc-Si:H cells on BR substrate (Fig. 3) are complex due to the texture of the BR, but the growth of the hill-like features can still be seen. New smaller size features appear on top of the large features of the 2 μm thick cell, which may indicate new nucleation of microcrystalline grains. Figure 4 plots the surface roughness, defined as the root mean square (RMS) value of the feature size, versus cell thickness of samples on BR and SS substrates. For the samples on SS, the roughness monotonically increases with increasing thickness, which is likely related to the evolution of the microcrystallites in the μc-Si:H film. For the cells on BR, the roughness also increases with thickness, but the total roughness is mainly dominated by the surface texture of the substrate.

Raman measurements (done by Daxing Han) show an increase of microcrystalline volume fraction from 60% for the 0.3 μm thick cell to 75% for the 2 μm thick cell. X-ray scattering diffraction (XRD) measurements have been done by the Don Williamson group and the results confirm the increase of microcrystalline volume fraction as a function of film thickness. Detailed results of Raman and XRD data will be reported by Daxing Han and Don Williamson, respectively.

In summary, we have investigated the effect of the texture of the substrate and film thickness on μc-Si:H solar cell performance. We found that the BR substrate has some influence on cell performance and material structure, but is not the main cause of low J_{sc} in thick μc-Si:H solar cells. We attribute the problem to the increase of microcrystalline volume fraction of μc-Si:H films with increasing film thickness. Based

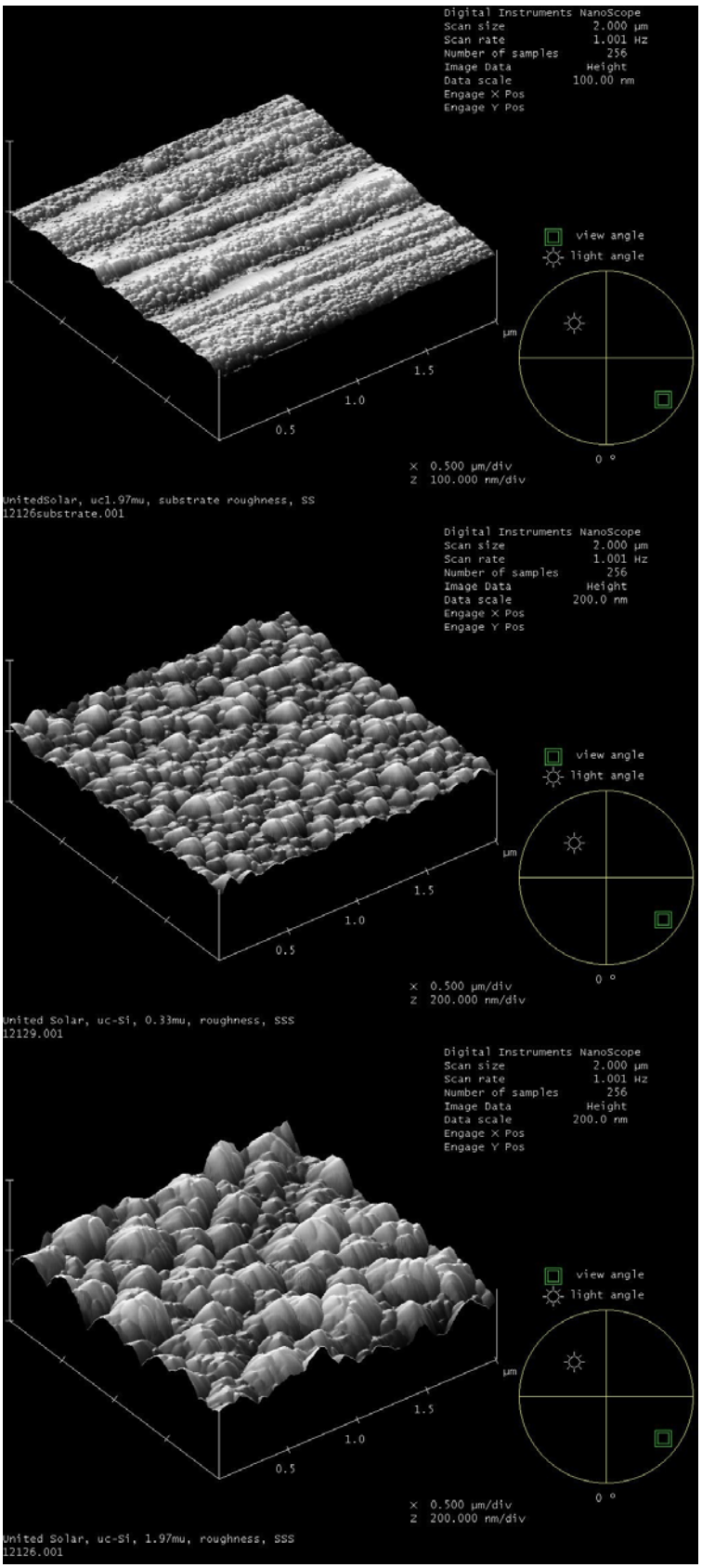

Figure 2. AFM images of (upper) a SS substrate, (middle) a 0.3 µm thick µc-Si:H solar cell and (bottom) a 2 µm thick µc-Si:H solar cell on SS substrate.

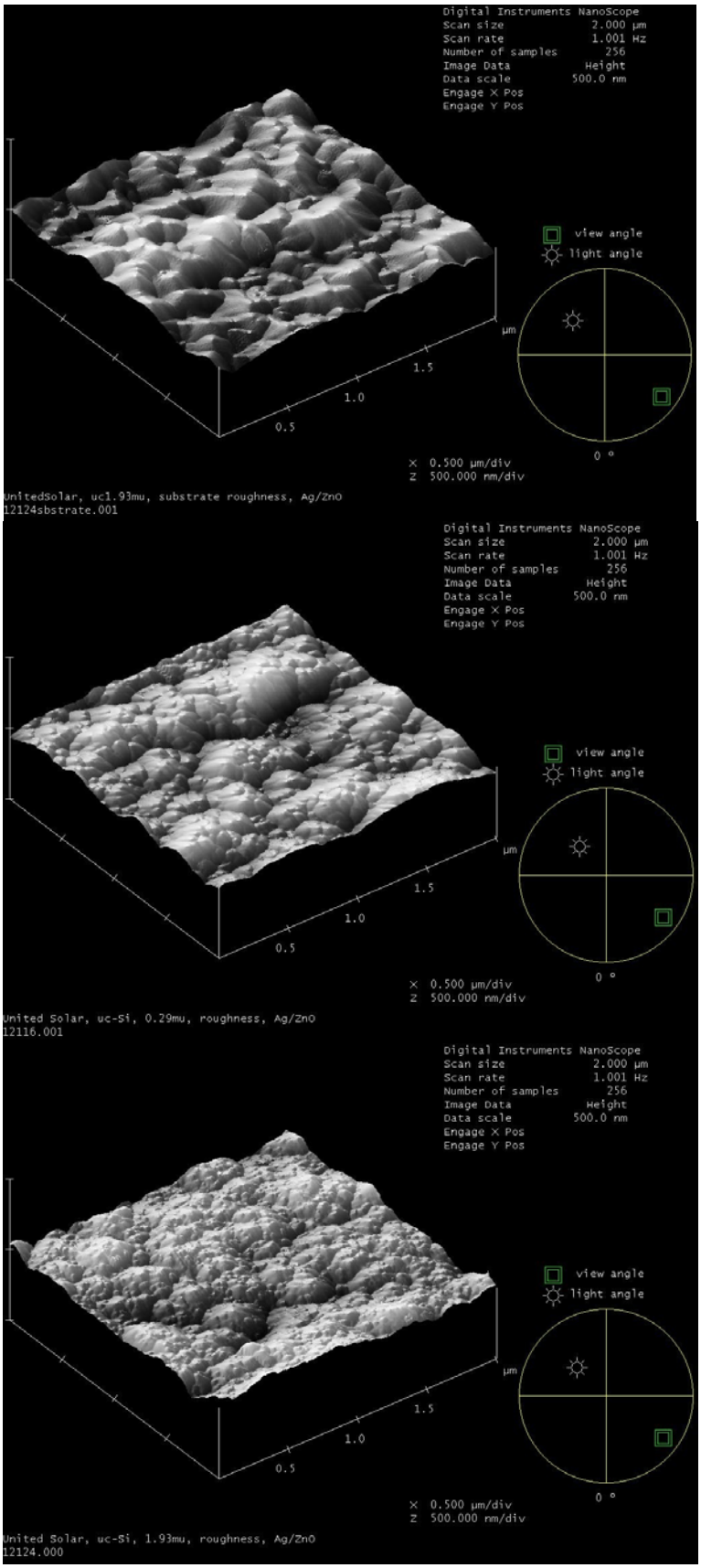

Figure 3. AFM images of (upper) a Ag/ZnO BR substrate, (middle) a 0.3 µm thick µc-Si:H solar cell, and (bottom) a 2 µm thick µc-Si:H solar cell on Ag/ZnO BR substrate.

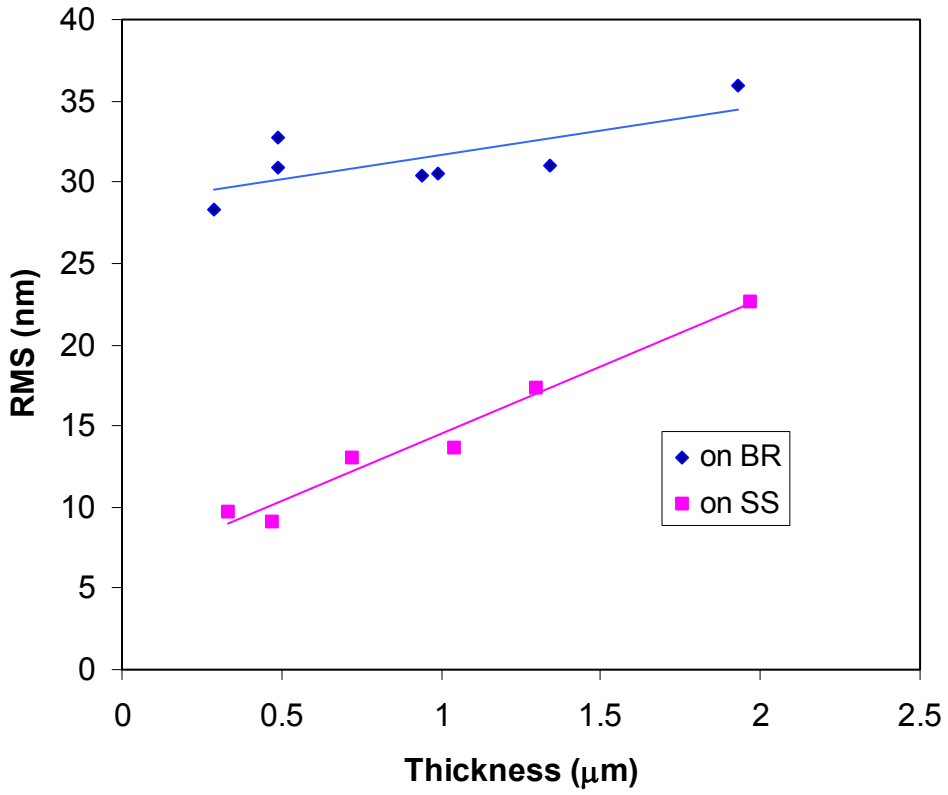

Figure 4. The surface roughness of the μc-Si:H solar cells versus the intrinsic layer thickness.

on these results, it appears that use of an optimized H_2 dilution profile to control the microcrystallite size and volume fraction during the deposition could lead to an improvement of thick μc-Si:H cell performance.

3. Hydrogen dilution profile for μc-Si:H single-junction cell

We made a series of μc-Si:H solar cells with profiled SiH_4 flow rates as shown in Fig. 5, where the H_2 flow rate and other deposition parameters were kept unchanged. The solar cells were deposited using MVHF on Ag/ZnO BR. We fixed the intrinsic layer thickness at ~2 μm since we have observed significant problems in cells with this thickness. Table IV lists a summary of the J-V characteristics of this series of solar cells. It appears that ramping up by 2 arbitrary units at each step leads to the best cell performance. The main increase is in J_{sc}. As shown in Fig. 6, the response in the middle and long wavelength region has been increased significantly for cells with 2 and 3 units/step. The ramping with 3 units/step shows the highest J_{sc}, but the FF is low due to the crossover of dark and light J-V, indicating a mixed phase material with high amorphous component near the *p/i* interface region. When the step is 4 units/step, the cell performance became very poor (a kink appears in the J-V curve) due to the increase of amorphous component near the *p/i* interface region.

In conclusion, a proper ramping of H_2 dilution has shown improvement on cell performance, especially in J_{sc}. From the increased quantum efficiency response in the middle and long wavelength region, we can conclude that the deterioration of cell performance for thick cells is due to the increase of the microcrystalline volume fraction, which may be associated with the increase of microvoid density. Too much ramping causes a mixed-phase state in the region near the *p/i* interface, and hence, poor cell performance.

Table IV. SiH_4 flow rates during the μc-Si:H intrinsic layer deposition and corresponding J-V characteristics of μc-Si:H solar cells made using MVHF glow discharge.

Sample No.	SiH_4 flow increase (arb. units)	Q (mA/cm^2)		V_{oc} (V)	FF			P_{max} (mW/cm^2)
		AM1.5	>610nm		AM1.5	Blue	Red	
12159	Flat	21.35	10.72	0.408	0.537	0.639	0.638	4.68
12162	1	22.03	11.42	0.411	0.545	0.651	0.634	4.93
12160	2	23.02	12.42	0.413	0.520	0.620	0.635	4.94
12165	3	24.03	13.54	0.413	0.436	0.560	0.591	4.33
12167	4	20.84	10.31	0.437	0.391	0.607	0.515	3.56

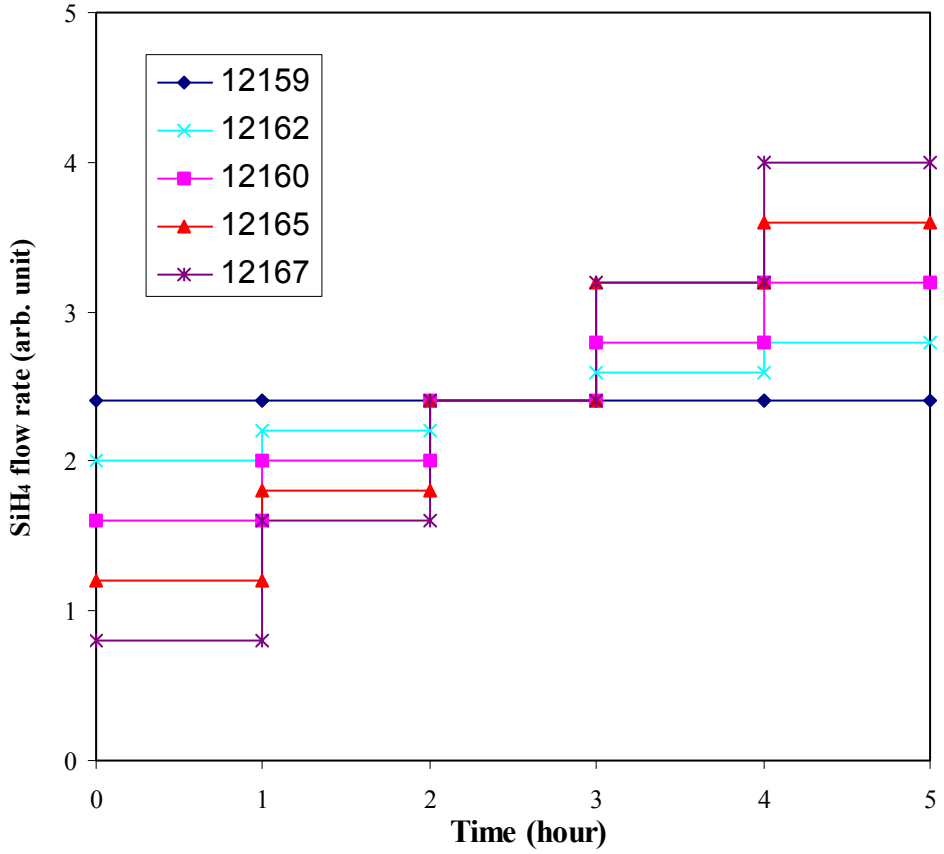

Figure 5. SiH_4 flow rate as a function of time for various H_2 dilution profiles. The H_2 flow rates were the same for all the samples.

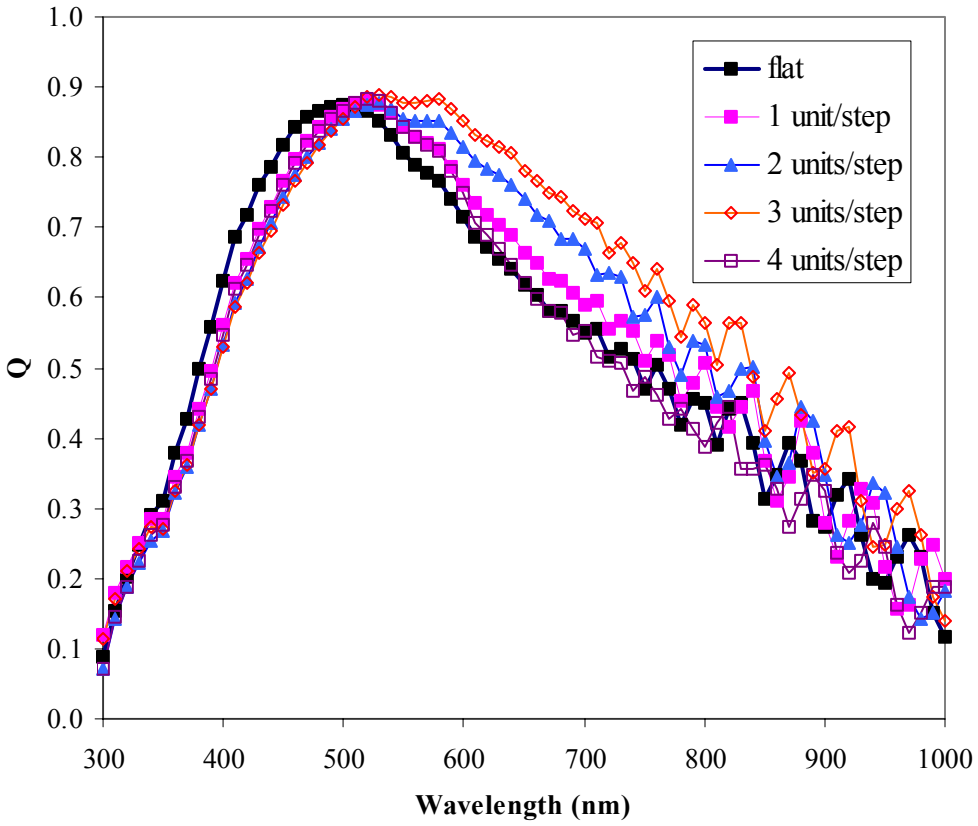

Figure 6. Quantum efficiency of microcrystalline silicon solar cells made with various SiH_4 flow rate profiles.

4. Optimization of microcrystalline silicon solar cells made using MVHF at high deposition rates

This section describes the optimization of a-Si:H/μc-Si:H double-junction solar cells prepared at a high deposition rate using MVHF glow discharge. A prerequisite is to develop a high quality μc-Si:H material and high performance μc-Si:H bottom cell. Previously, we have reported an initial active-area efficiency of 7.1 % using a μc-Si:H single-junction structure, where the intrinsic μc-Si:H layer was deposited in 50 minutes. The corresponding parameters were V_{oc}=0.503 V, J_{sc}=22.83 mA/cm^2, and FF=0.611. The main limitation to obtaining higher efficiency was low FF. As shown in the previous sections, FF critically depends on the microstructure of the material. If the material contains more microvoids or cracks, it may result in more defects related to oxygen contamination and grain boundaries. To obtain μc-Si:H material with a highly dense structure, the strategy is to make the material at the transition region from μc-Si:H to a-Si:H. Table V lists three μc-Si:H single-junction solar cells made according to this idea. We have achieved a conversion efficiency of 7.7 % for sample 12255, which is a new record for μc-Si:H solar cells made by the VHF technique. Figure 7 shows the corresponding J-V characteristics and quantum efficiency. For sample 12254 with a deposition time of 60 minutes, the V_{oc} is 0.549 V and FF 0.696, indicative of a high quality material. In a manufacturing environment, a shorter deposition time is more desirable. For sample 12274, we reduced the deposition time to 40 min. and obtained an efficiency of 6.9%. Incorporating this cell into a double-junction structure, a conversion efficiency of 11.9 % has been achieved as shown in Fig. 8. This efficiency is superior to the previous record of 11.4% for cells made with the same bottom cell deposition time.

Table V. J-V characteristics of three μc-Si:H solar cells made using MVHF glow discharge at high deposition rates.

Sample No.	Time (min)	V_{oc} (V)	FF	J_{sc} (mA/cm^2)	P_{max} (mW/cm^2)
12274	40	0.498	0.641	21.51	6.9
12254	60	0.549	0.696	19.51	7.5
12255	80	0.528	0.683	21.33	7.7

5. High rate μc-Si:H cell deposition using RF glow discharge

As reported in literature, successful methods for high rate deposition of μc-Si:H films are VHF glow discharge and RF glow discharge under high pressure and high power. As an industrial R&D group, we need to evaluate both methods and study the feasibility of each method for manufacturing purpose. We have made significant effort on the deposition of μc-Si:H solar cells using MVHF and obtained good results as reported in the previous sections and the Phase I report. In this quarter, we started the study of μc-Si:H solar cells using RF glow discharge under high pressure and high power.

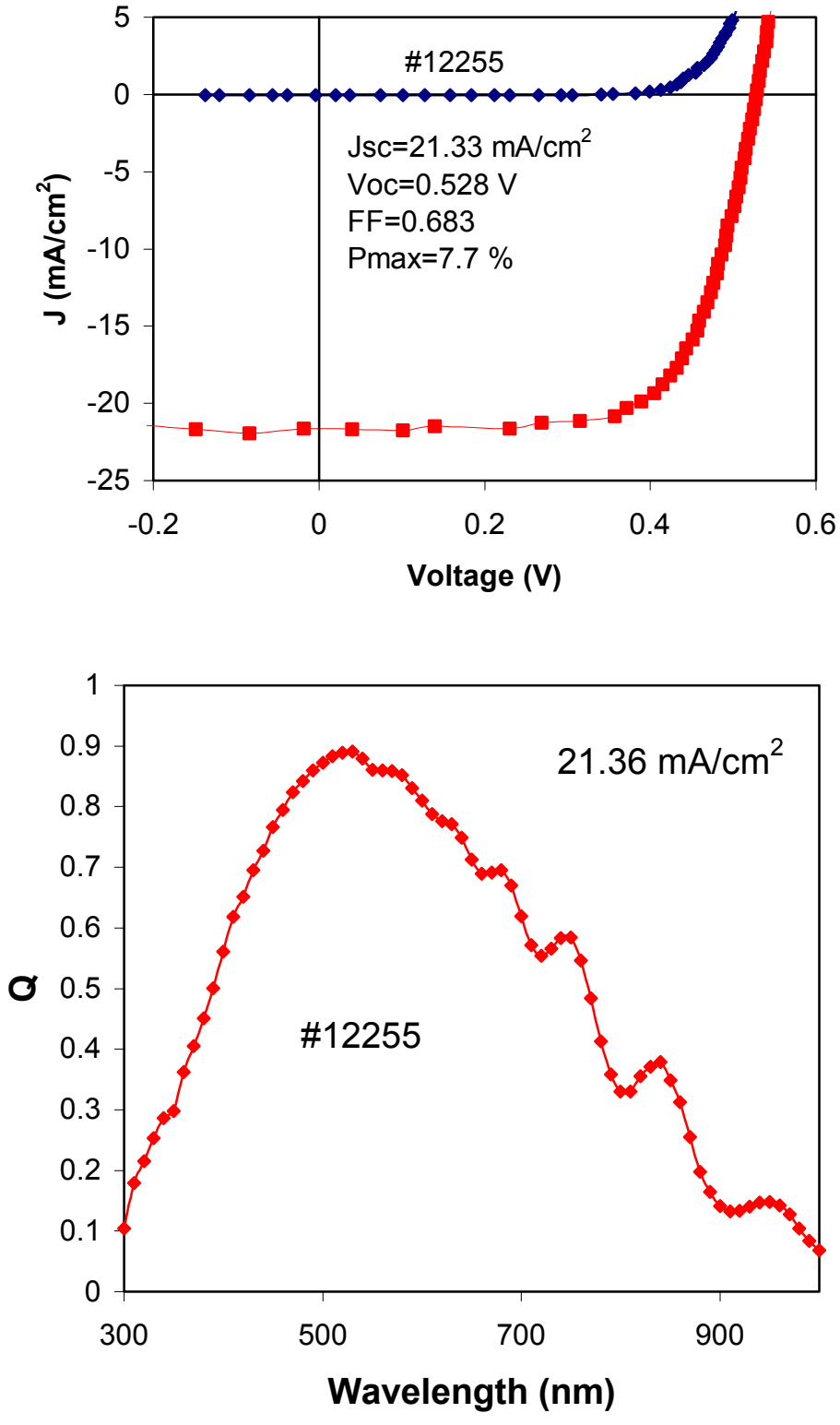

Figure 7. (upper) J-V characteristics and (bottom) quantum efficiency of the best μc-Si:H single-junction solar cell made with MVHF glow discharge.

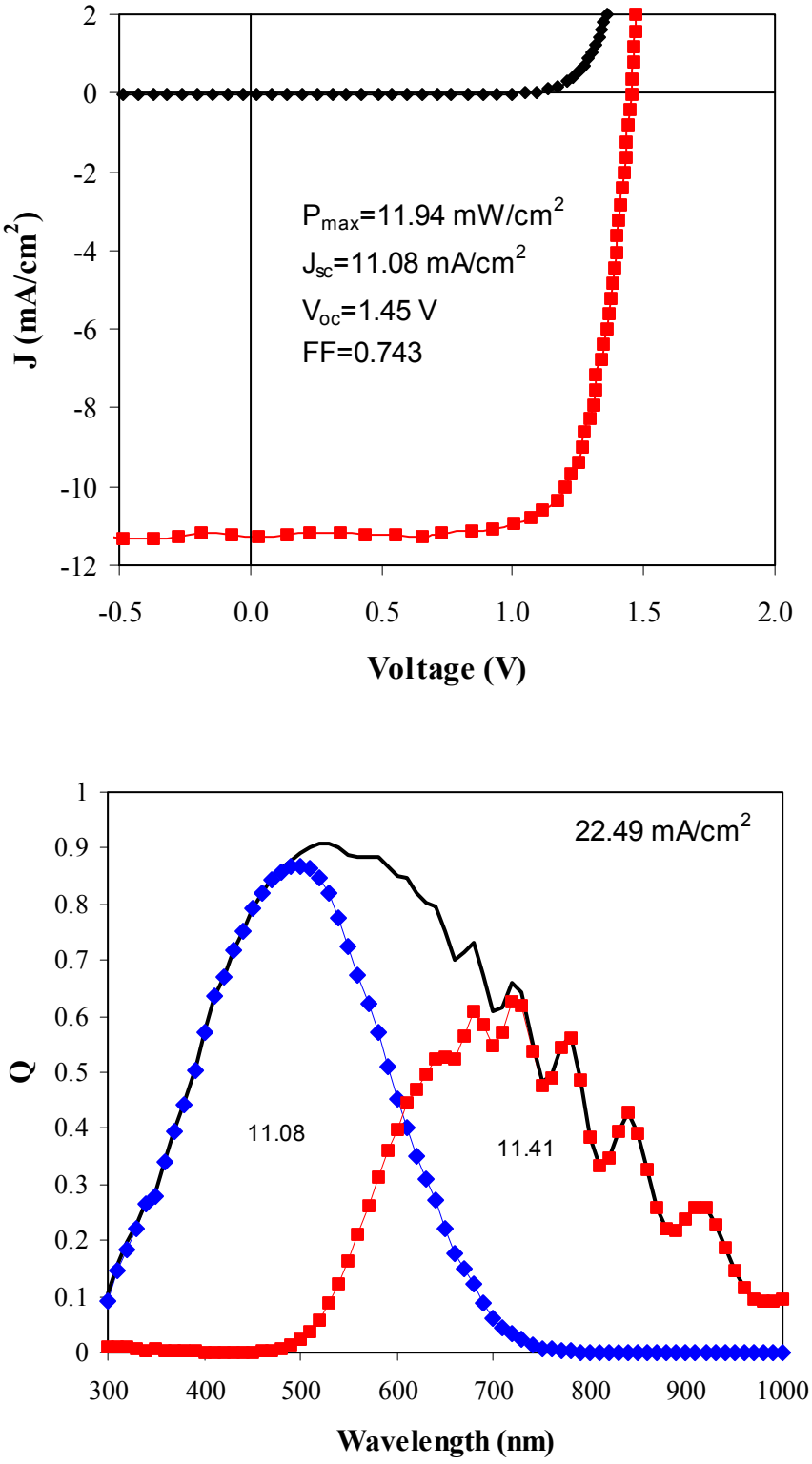

Figure 8. (upper) J-V characteristics and (bottom) quantum efficiency of an a-Si:H/µc-Si:H double-junction solar cell made using MVHF with µc-Si:H intrinsic layer deposition time of 40 minutes.

A multi-chamber RF glow discharge system has been used for μc-Si:H solar cell deposition. Single-junction μc-Si:H *n-i-p* cells were deposited on Ag/ZnO back reflector coated stainless steel substrate. The doped layers were deposited using the same optimized conditions. We searched in parameter space for the intrinsic μc-Si:H layer deposition, including hydrogen dilution, substrate temperature, RF power and pressure. We found that higher hydrogen dilution is required to reach the transition from amorphous to microcrystalline phase under high pressure than under low pressure. High substrate temperature helps to reduce the required hydrogen dilution, but the good solar cells were made at relatively low temperature but with high hydrogen dilution.

As expected, the high pressure RF glow discharge suffered uniformity problem. The cell performance is not uniform on 2×2 in^2 substrate. Table VI lists the J-V characteristics of solar cells at different locations on the substrate. It appears that the cells in the center have high V_{oc} but low J_{sc}, indicating a low microcrystalline volume fraction in the center. The highest efficiency for single-junction μc-Si:H cells is 6.7%, in which the intrinsic layer was deposited in 60 minutes. Figure 9 shows the J-V characteristics and quantum efficiencies of cells in the center and at the edge. From the quantum efficiency plot, one can see the long wavelength response is higher for the cell on the edge than in the center. The uniformity depends not only on pressure, but also on other parameters such as gas flow and RF power. Currently we are working on the optimization of deposition conditions to achieve high efficiency and uniform solar cell deposition at high rate.

We used the RF high rate μc-Si:H cell as the bottom cell in an a-Si:H/μc-Si:H double-junction structure and achieved an initial active-area efficiency of 12.3%, where the bottom cell μc-Si:H layer was deposited in 2 hours. Table VII lists the J-V characteristics of three cells made with different bottom cell deposition times and Fig. 10 plots the J-V characteristics and quantum efficiency of the best a-Si:H/μc-Si:H double-junction cell.

In summary, we have started RF glow discharge deposition of μc-Si:H solar cells under high pressure with high power at high deposition rate. We achieved an initial active-area efficiency of 6.7% with a μc-Si:H single-junction cell and 12.3% with an a-Si:H/μc-Si:H double-junction cell. Currently we face the uniformity problem. Further optimization of the cell performance and uniformity are under way.

Table VI. Initial active-area J-V characteristics of μc-Si:H single-junction cells made with RF under high pressure at high rate. The μc-Si:H deposition time was 60 minutes.

Sample #	Position	Eff (%)	J_{sc} (mA/cm^2)	V_{oc} (V)	$FF_{AM1.5}$	FF_{blue}	FF_{red}
7693	Center	6.6	21.44	0.517	0.598	0.662	0.670
	Edge	6.3	22.10	0.497	0.573	0.639	0.638
	Corner	5.6	23.60	0.468	0.509	0.604	0.601
7699	Center	6.7	22.48	0.494	0.605	0.651	0.604
	Edge	6.5	23.57	0.474	0.580	0.624	0.597

Table VII. Initial active-area J-V results of a-Si:H/μc-Si:H double-junction cells made with RF glow discharge under high pressure at 3 Å/s. t is the μc-Si:H deposition time.

Sample #	t (min)	Eff (%)	J_{sc} (mA/cm^2)		V_{oc} (V)	FF
			Top	Bottom		
7727	60	10.0	12.38	9.60	1.439	0.722
7742	90	11.9	11.82	11.63	1.403	0.730
7741	120	12.3	11.89	12.69	1.410	0.731

6. Large area deposition

The principal objective of the large-area deposition work is to develop an improved recipe for the 30 MW/year production line to produce high efficiency solar modules. Therefore, the hardware design, deposition rate, and reactive gas should be consistent. In the last quarterly report, we completed the installation of new RF cathodes in three deposition chambers of the large area 2B machine. Experimental results showed that the thickness uniformity of various layers deposited using the new cathodes is superior to that obtained with the previous cathodes. The uniformity of device performance for the component cells was also improved. In this quarter, we continued to work on the optimization of component cells and started to make a-Si:H/a-SiGe:H/a-SiGe:H triple junction solar cells using the improved large-area 2B machine.

Triple-junction solar cells were deposited on Al/ZnO coated stainless steel. The growth conditions are under the constraints of the requirements of the 30 MW/year production machine. The deposition rate is ~ 3 Å/s. We have also targeted replacing Si_2H_6 and GeH_4 gas mixture with SiH_4 and GeH_4 gas mixture for the fabrication of the middle and bottom cells. SiH_4 is cheaper than Si_2H_6 and, therefore, successful substitution of Si_2H_6 with SiH_4 will reduce the production cost. Table VIII lists the initial performance of the best a-Si:H/a-SiGe:H/a-SiGe:H triple-junction solar cell fabricated using SiH_4 and GeH_4 gas mixture for the middle and bottom cells. The 2" × 2" cells were cut from a large-area substrate and 0.25 cm^2 ITO dots were deposited on top of the cells as top contact. The active-area efficiency for this sample is in the range of 11.0-11.4 % with an average value of 11.2 %. The standard deviation is 0.16. The cell LC1 exhibits the best initial active-area conversion efficiency of 11.43 %. The J-V characteristics and quantum efficiency of the device are shown in Fig. 11. The cell performance is close to our previous record of 11.7% made using Si_2H_6 and GeH_4 mixture. Further optimization of deposition conditions and fabrication of large-area modules are under way.

Table VIII. Initial performance of a-Si:H/a-SiGe:H/a-SiGe:H triple-junction solar cells made using the improved 2B machine with SiH_4 and GeH_4 mixture.

Sample	Substrate	Area	Efficiency	J_{sc}	V_{oc}	FF	R_s
2B9423		(cm^2)	(%)	(mA/cm^2)	(V)		Ω cm^2
N	AlZnO	0.25	11.14	6.39	2.287	0.762	28.1
LC1	AlZnO	0.25	11.43	6.82	2.238	0.749	27.7
S	AlZnO	0.25	11.09	6.41	2.259	0.766	28.2
Average			**11.22**	**6.54**	**2.261**	**0.759**	**28.0**
Standard Deviation			**0.16**	**0.20**	**0.02**	**0.007**	**0.22**
Coefficient of Variation			**1.44 %**	**3.06 %**	**0.89 %**	**0.92 %**	**0.77 %**

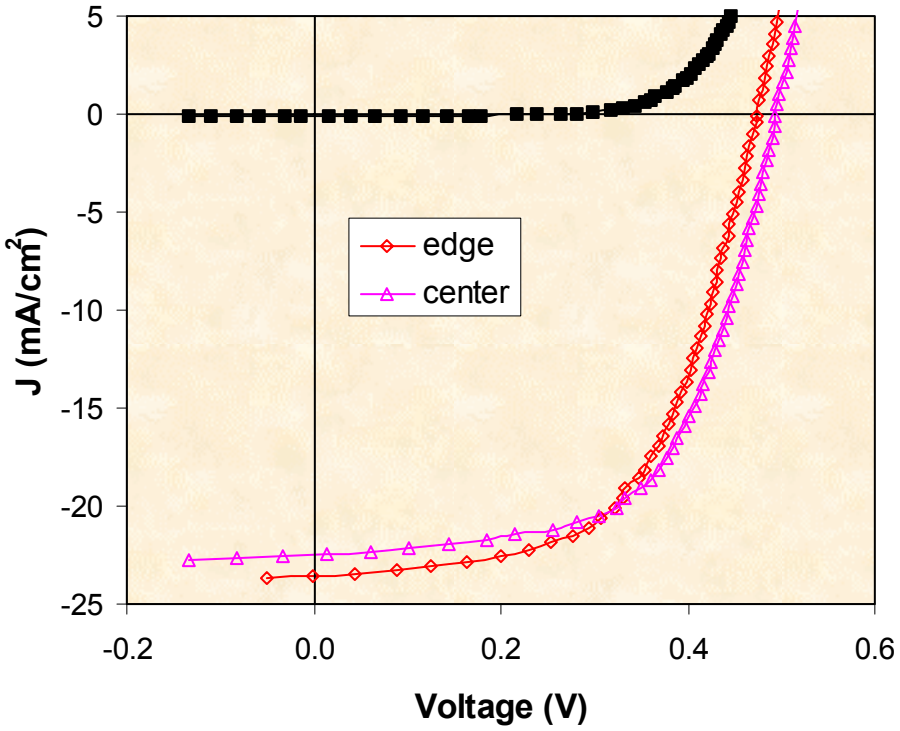

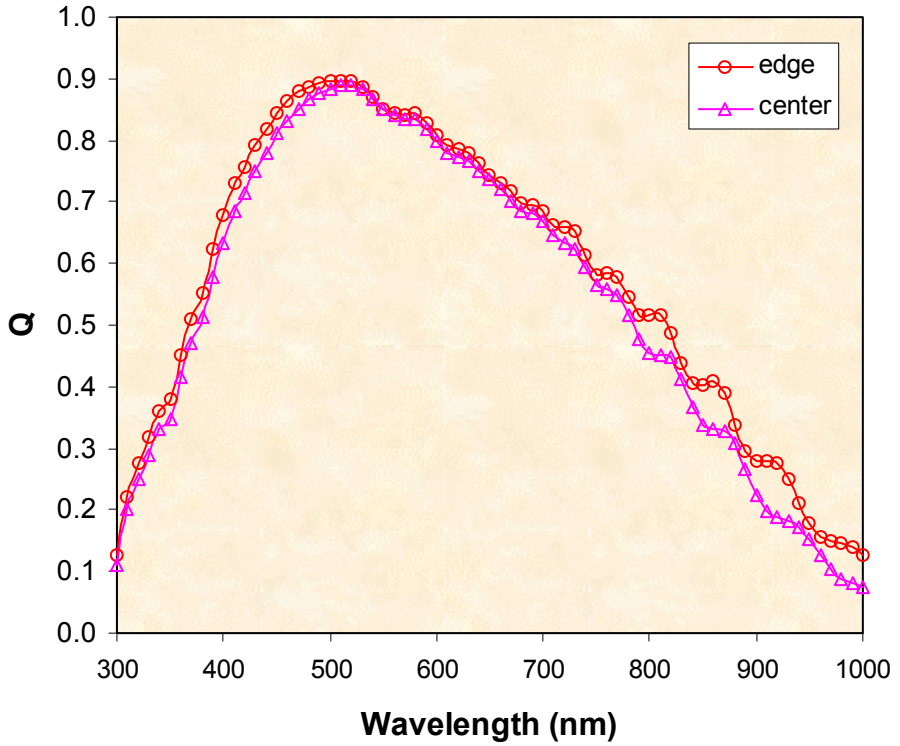

Figure 9. J-V characteristics and quantum efficiency of μc-Si:H single-junction cells at the center and the edge of the substrate. The μc-Si:H layer was deposited using high pressure RF glow discharge at ~ 3 Å/s for 60 minutes.

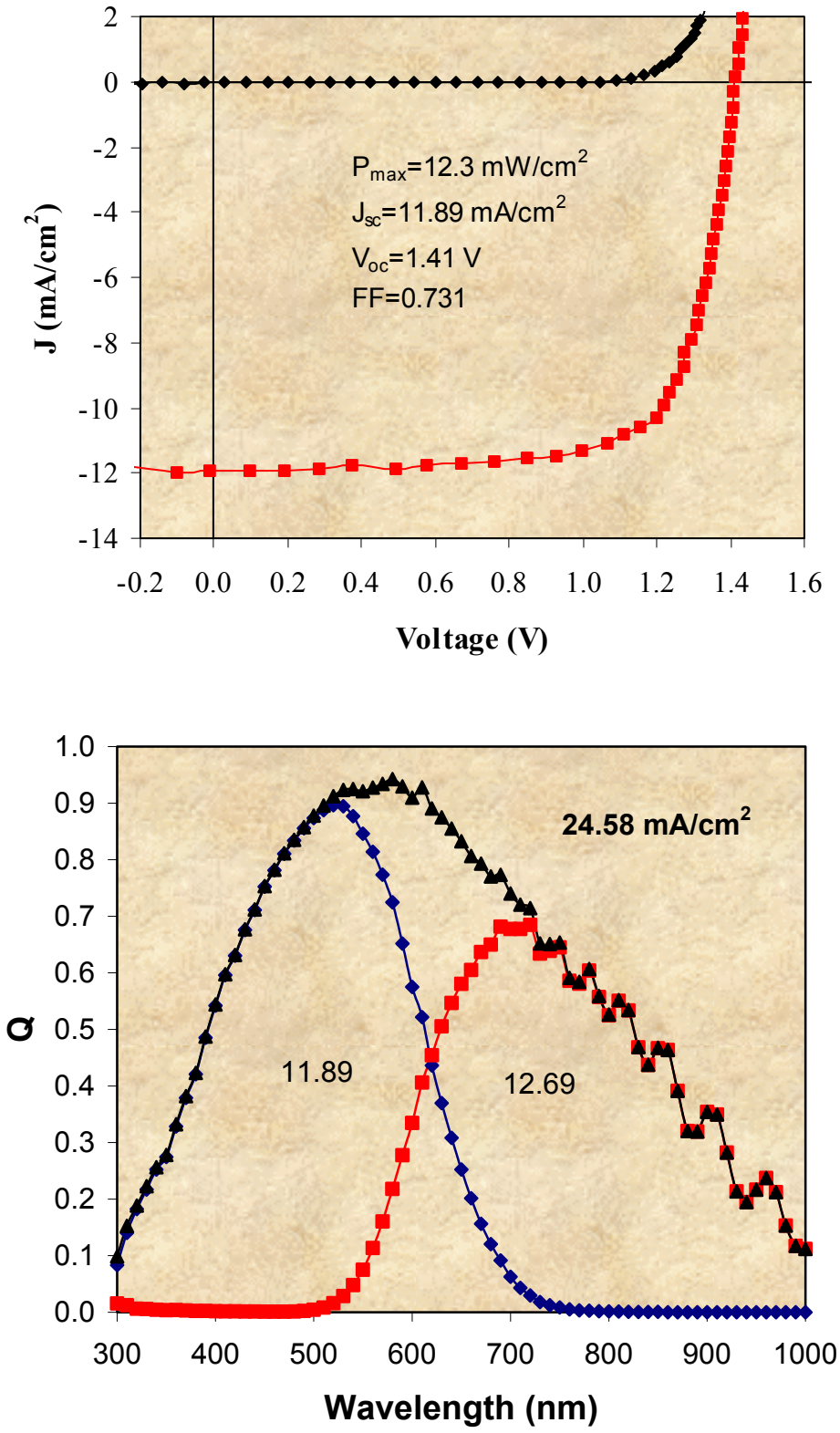

Figure 10. (upper) J-V characteristics and (bottom) quantum efficiency of an a-Si:H/µc-Si:H double-junction cell deposited using high pressure RF glow discharge at ~ 3 Å/s.

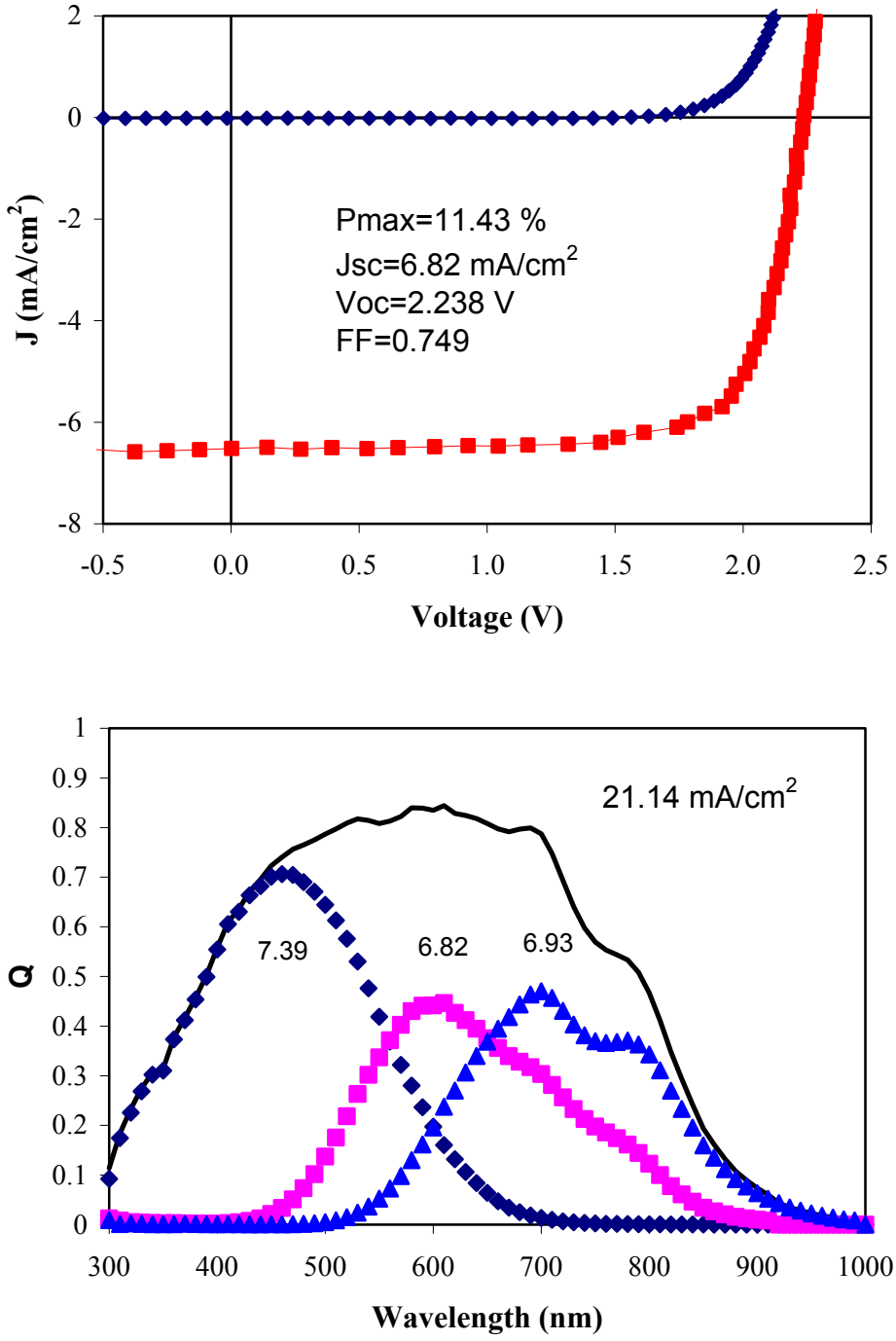

Figure 11. J-V characteristic and quantum efficiency of the best a-Si:H/a-SiGe:H/a-SiGe:H triple-junction solar cell made using 2B machine under production constraints with SiH_4 and GeH_4 gas mixture.

7. Summary

We have systematically studied the thickness dependence of μc-Si:H single-junction solar cells deposited on both specular stainless steel substrate and textured Ag/ZnO back reflector. The results show that the increase of microcrystalline volume fraction is the main cause of low J_{sc}. The mechanism for this problem could be the increase of microvoid/microcrack density with the increase of microcrystalline volume fraction, especially the growth of the (220) orientation. Detailed analysis of the material properties by Raman and XRD support this conclusion.

By profiling H_2 dilution, we have improved the J_{sc} significantly. We have succeeded in suppressing the increase of microcrystalline volume fraction and reducing the problems associated with the increase of microvoid density.

On high rate deposition, we continued to optimize the MVHF glow discharge conditions and achieved an initial active-area efficiency of 7.7% single-junction cell, which is higher than the previous record of 7.1%. Using the improved condition, we obtained an initial active-area efficiency of 11.9% with an a-Si:H/μc-Si:H double-junction structure, where the bottom cell μc-Si:H intrinsic layer deposition time was 40 minutes. We started μc-Si:H solar cell deposition using RF glow discharge under high pressure with high power and achieved an initial active-efficiency of 12.3% with an a-Si:H/μc-Si:H double-junction structure.

On large-area solar cell deposition, we continued to work on the a-Si:H/a-SiGe:H/a-SiGe:H triple-junction solar cells using SiH_4 and GeH_4 gas mixture for a-SiGe:H layer deposition under production constraints. The solar cells are deposited on Al/ZnO back reflector from the production line. We have achieved an initial active-area efficiency of 11.4%, which is close to the best cell made under similar conditions but using Si_2H_6 and GeH_4 mixture. Currently, we are working on the fabrication of modules using the optimized recipe.

8. References

[1] K. Yamamoto, A. Nakajima, M. Yoshimi, T. Sawada, S. Fukuda, K. Hayashi, T. Suezaki, M. Ichikawa, Y. Koi, M. Goto, T. Sasaki, and Y. Tawada, Proc.of 3rd World Conference on Photovoltaic Energy Conversion, Osaka, Japan, May 11-18, 2003.

[2] K. Saito, M. Sano, H. Otoshi, A. Sakai, S. Okabe, and K. Ogawa, Proc.of 3rd World Conference on Photovoltaic Energy Conversion, Osaka, Japan, May 11-18, 2003.